International Journal of Science and Research (IJSR)
ISSN (Online): 2319-7064
Index Copernicus Value (2015): 78.96 | Impact Factor (2015): 6.391

Using Finite Element to Modify Winkler Model for Raft Foundation Supported on Dry Granular Soils

Salah R. Al-Zaidee[1], Aqeel T. Fadhil[2], Omar K. Al-Kubaisi[3]

[1, 2, 3]The University of Baghdad, College of Engineering, Civil Eng. Department, Baghdad, Iraq

Abstract: ***Winkler foundation is a traditional model that is usually adopted in structural engineering to simulate the stiffness of underneath soil as decoupled springs with spring constant determined based on plate load test or based on a correlation with soil bearing capacity. This model leads to a fourth order differential equation. Analytical methods are usually adopted to solve the differential equation for regular loads and ideal boundary conditions while numerical methods, finite difference or finite element, are used to solve it for general loads and/or complex boundary conditions. The main drawback of Winkler model is neglecting or at best implicitly including, when spring constant is determined from correlation with soil bearing capacity, the interaction between adjacent soil prisms. This is in contrast with soil models adopted in geotechnical engineering which recognize soil shear strength and shear interaction between adjacent soil prisms. An abrupt change in soil subgrade reaction is usually seen under concentrated loads when using Winkler foundation and this change may be greater than the allowable soil capacity. With this situation, it is hard to compare the global behavior simulated by soil bearing capacity with the local behavior in the neighborhood of point loads. In this paper, raft foundations with regular columns arrangement, and supported by different underneath cohesionless dry soil profiles have been simulated using traditional Winkler foundation model and 3D finite element models. Linear regression models have been adopted to modify the results of Winkler model to take into account the aforementioned parameters. With these modifications, designers can preserve the benefits of Winkler foundation model, usually available in commercial software, while overcoming its drawbacks. Linear regression analyses applied on the results obtained from the two models show that two soil simulations are significantly correlated with correlation factors in the range of 0.9. The explanatory parameters adopted in regression analysis were raft dimensions, raft thickness, and material properties for both soil and concrete.***

Keywords: Winkler Foundation Model, Raft Foundation, Finite Element Model, Granular Soil

1. Introduction

One of the earliest models that simulate the soil flexibility beneath the foundation is the Winkler model. This model simulates the soil as a series of uncoupled elastic linear springs, that is, the deformations do not affect the neighboring springs. Winkler foundation was first introduced in 1867 by Dr. E. Winkler professor at the Technical University in Prague, see [1]. Since then, Winkler foundation has been widely used among structural and geotechnical engineers due to its reliability and convince [2]. However, the lack of including the shear coupling between the adjacent soil prisms somewhat reduces the efficiency of Winkler model and makes the engineers favor the use of finite element soil simulation for the sake of obtaining results that are more precise.

The divergence between the results obtained from Winkler model and those obtained from actual soil behavior becomes clearer when soil is subjected to concentered point or line loads. Consider for example a raft shown in Figure 1 where soil reactions are concentrated at supporting columns and high shear forces are generated in soil mass there. For this type of foundation, Winkler assumption seems unrealistic and may lead to adopt deep foundation due to the localized overestimated stresses under point loads.

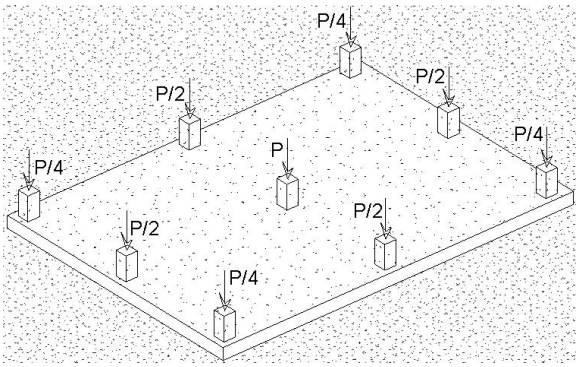

Figure 1: Raft foundation subjected to column concentrated loads

The goal of this study is to modify Winkler model to develop a more accurate, yet a simple linear model, that include the shear coupling and interaction between nearby soil particles.

2. Finite Element Modeling

Finite element models for different case studies are prepared in terms of parameters indicated in Figure 2.

Paper ID: ART20171997 DOI: 10.21275/ART20171997

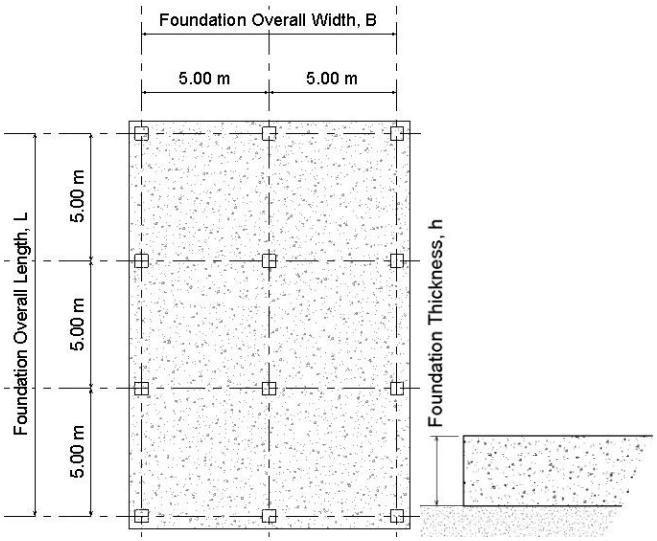

Figure 2: Case study parameters

2.1 Geometry and element types

For each case study, two models are adopted. In the first model, soil is simulated through Winkler springs, Figure 3, while a brick element is used to simulate soil mass for the second model, Figure 4. In the second model, underneath soil is isolated from semi-infinite soil mass at distance equal to overall foundation width "B" from each side of the footing and at a depth of 2B. According to the theory of elasticity, about 50% of stresses due to uniform surface loads can be accommodated within these boundaries [3].

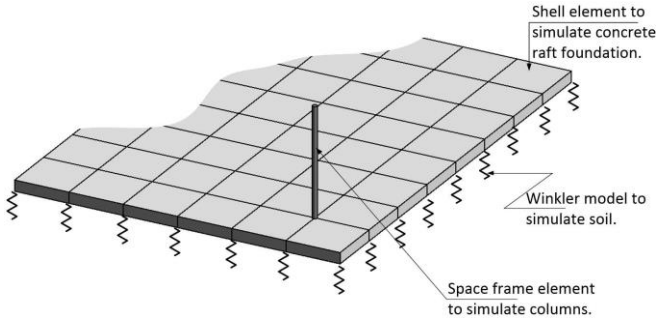

Figure 3: Finite element model with Winkler Foundation

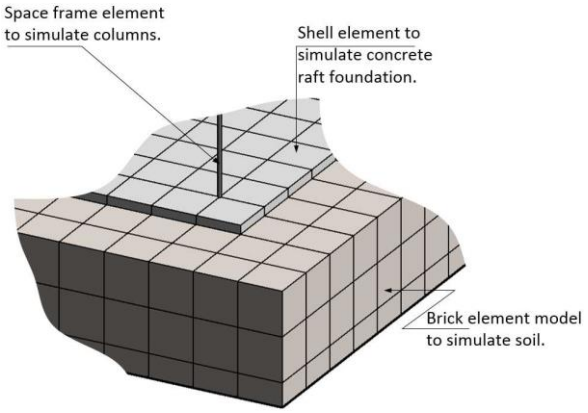

Figure 4: Finite element model with brick element to simulate soil

In both models, space frame element is used to simulate the elastic concrete columns where point loads are acting, while shell element is used to simulate the raft foundation.

A mesh size not greater than 0.5m is adopted in the finite element models for shell and brick element. This size is adequate to capture main features of the behavior [4]. With finite element discretization, equilibrium, compatibility, and constitutive relations for columns, raft foundation, and Winkler springs or soil mass are represented by (1) below:

$$[K]_{n\times n}\{d\}_{n\times 1}=\{f\}_{n\times 1} \quad (1)$$

where:

n is the total DOF for the system which is equal to: $dof_{per\ node}\times No.of\ Nodes$.

$[K]$ is the global stiffness matrix generated from elements stiffness assemblage according to a direct stiffness algorithm.

$\{f\}$ is the consistent nodal load vector that is determined from the applied loads.

2.2 Boundary conditions

With Winkler springs, stiffness matrix, K, of (1) above is already positive definite and has a unique solution [5]. While based on soil simulation with brick element, the stiffness matrix is semi-definite and boundary conditions should be added for stable system. Therefore, all translational DOF located on virtual sides and bottom surface where soil is isolated are restrained to obtain a positive definite stiffness matrix and to simulate the vanish of soil deformations at regions far from the loaded raft.

2.3 Material properties

Concrete and soil are both simulated as linear isotropic materials that obey Hooke's law. Two parameters, namely, elastic modulus, E, and Poisson ratio, ν, are defined while shear modulus, G, has been determined from the following relation between the three elastic parameters, [6]:

$$G=\frac{E}{2(1+\nu)} \quad (2)$$

According to [7], concrete elastic modulus, E_c, is determined based on (3) below, while a Poisson ratio of 0.2 has been adopted according to recommendation of [8] for stresses far from concrete collapse stage.

$$E_c=4700\sqrt{f_c^{'}} \quad (3)$$

where $f_c^{'}$ is cylindrical compressive strength of concrete in MPa. A value of 28 MPa is adopted in this study.

As it is difficult to gather undisturbed specimens for cohesionless soils, their stiffness and strength properties are usually related to the results of the standard penetration test, SPT [3]. According to [9], elastic modulus of granular soils can be related to standard penetration number, N, based on following relation:

$$E_s=10p_aN \quad (4)$$

where p_a is the atmospheric pressure, approximately equal to $100\,kPa$.

According to [9], Poisson ratio for cohesionless soils, ν_s, can be related to its angle of internal friction, ϕ, based on (5) below. While [10] recommend the relation indicated in (6)

Paper ID: ART20171997 DOI: 10.21275/ART20171997

below to correlate the angle of internal friction, ϕ, to SPT value. Two equations indicate an indirect relation between soil Poisson ratio, ν_s, and SPT values.

$$\nu_s = 0.1 + 0.3\left(\frac{\phi - 25}{20}\right) \quad (5)$$

$$\phi = 27.1 + 0.3N - 0.00054(N)^2 \quad (6)$$

According to [11], coefficient of subgrade reaction, k_s, can be related to soil allowable bearing capacity, $q_{allowable}$, based on (7) below.

$$k_s = 40\, FS\, q_{allowable} \quad (7)$$

Soil allowable bearing capacity is either determined based on requirements of global shear failure or based on local shear failure and settlement failure [12]. Due to its dimensions, allowable bearing capacity for raft foundation is usually determined based on settlement requirements [13].

According to [9], allowable bearing capacity for cohesionless soils can be related to SPT value based on the following relation:

$$q_{allowable} = \frac{N}{0.08} \times \left(\frac{S_e}{25}\right) \quad (8)$$

where S_e is the allowable settlement in mm.

As raft footings are relatively rigid and can bridge possible pockets in soil mass, an allowable settlement in the range of 50mm is usually recommended [14]. Based on this settlement range, (8) above is reduced to the formula indicated in (9) below:

$$q_{allowable} = 25\, N \quad (9)$$

2.4 Applied loads

As indicated in Figure 1, all applied loads are concentrated column loads. Loads with this nature can simulate practical problems and emphasize the role of shear force between soil prisms that are neglected using Winkler model and included through soil mass models.

Loads are assumed proportional, where axial load on an interior column is twice the axial load acting on edge columns and four times the load acting on corner columns. The proposed load proportionality indirectly reflects the stiffness of superstructure and compensates its absence from the finite element models of this study [14].

3. Dimensional Analysis

3.1 Basic Relations

Related literature indicate that the distribution of subgrade reaction is a function of the stiffness of raft foundation and the stiffness of the supporting soil [15]. Soil stiffness is a function of its elastic modulus, E_s, angle of internal friction, ϕ, and Poisson ratio, ν_s. The elastic modulus, E_s, and the angle of internal friction, ϕ, both can be expressed in terms of the coefficient of subgrade reaction, k_s. On the other hand, foundation stiffness can be expressed in terms of foundation dimensions, B and L, foundation thickness, h, concrete elastic modulus, E_c, and concrete Poisson ratio , ν_c.

Considering the aforementioned parameters, problem dependent and independent variations can be expressed in terms of functions f and g presented in (10) and (11) below.

$$\frac{q_1}{q_2} = f\left(E_c, \frac{\nu_c}{\nu_s}, k_s, L, B, h\right) \quad (10)$$

$$\frac{M_1}{M_2} = g\left(E_c, \frac{\nu_c}{\nu_s}, k_s, L, B, h\right) \quad (11)$$

where: q_1 and M_1 are respectively the maximum subgrade reaction and foundation maximum bending moment determined with three-dimensional soil simulation. q_2 and M_2 are respectively the maximum subgrade reaction and foundation maximum bending moment determined with Winkler soil simulation.

As raft foundation is usually designed as an isotropic slab to avoid possible differential settlement, therefore locations where maximum settlement and maximum moment occur are not included in the basic relations [16].

In the sub articles below, dimensional analysis is used to rewrite (10) and (11) above in term of dimensionless groups. With these dimensionless groups, analysis is simplified as the number of variables is reduced and the case studies are ensured to be significantly different.

3.2 Number of independent dimensionless groups

According to π theorem, [17], *the number of independent groups that may be employed to described a phenomenon known to involve n variables is equal to $n-r$, where r is the number of basic dimensions needed to express the variables dimensionally*.

For this study, as all variables can be expressed in terms of force dimension, F, and length dimension, L, therefore r is two and number of dimensionless groups is:

$$n - r = 5 - 2 = 3 \quad (12)$$

3.3 Dimensionless Groups

Let the relation in (10) above be continuous and with adopting first terms of its infinite series expansion, dimensional relation indicated in (13) below is obtained:

$$0 = \left(\frac{F}{L^2}\right)^a \left(\frac{F}{L^3}\right)^b (L)^c (L)^d (L)^e \quad (13)$$

Paper ID: ART20171997 DOI: 10.21275/ART20171997

By equating both sides of (13) above according to the law of dimensional homogeneity, the following set of simultaneous equations is formulated:

For force F:

$$a+b=0 \qquad (14)$$

For length L:

$$-2a-3b+c+d+e=0 \qquad (15)$$

It can be shown simply that following dimensionless groups satisfy above equations.

$$a=-b$$

$$c=b-d-e$$

In terms of dimensionless groups, (10) above would be as indicated in (16) below.

$$\frac{q_1}{q_2}=\left(\frac{k_s\times L}{E_c}\right)^b\left(\frac{\nu_c}{\nu_s}\right)\left(\frac{B}{L}\right)^d\left(\frac{h}{L}\right)^e \qquad (16)$$

In the same approach, non-dimensional relations for maximum bending moment in the raft foundation is presented in (17) below.

$$\frac{M_1}{M_2}=\left(\frac{k_s\times L}{E_c}\right)^{b'}\left(\frac{\nu_c}{\nu_s}\right)\left(\frac{B}{L}\right)^{d'}\left(\frac{h}{L}\right)^{e'} \qquad (17)$$

As indicated in below, based on data generated from finite element analyses, a regression analysis is used to determine the coefficients b' through e'.

4. Case Studies and Results

With referring to Figure 2, parameters for different case studies and the corresponding results for two types of finite element simulations are presented in Table 1 and Table 2, where:

σ_{zz} is soil pressure based on simulation of soil mass,

M_{xx} is bending moment that produces stresses along foundation length, L,

M_{yy} is bending moment that produces stresses along foundation width, B.

Table 1: Parameters for case studies and the corresponding results of Soil Mass model

Input Data			*Results (Soil Mass)*		
N_{60}	*L* (m)	*B* (m)	σ_{zz} (kN/m^2)	M_{xx} (kN.m/m)	M_{yy} (kN.m/m)
10	10	10	47.68	-398.81	-398.81
10	20	10	47.89	-403.87	-409.69
10	30	10	48.44	-384.65	-410.28
10	40	10	48.79	-384.93	-410.41
10	50	10	48.70	-385.07	-410.55
20	10	10	46.11	-388.15	-388.15
20	20	10	48.83	-377.09	-396.20
20	30	10	48.91	-372.20	-396.56
20	40	10	48.46	-372.40	-396.64
20	50	10	48.44	-372.44	-396.70
30	10	10	45.90	-380.93	-380.93
30	20	10	49.83	-367.25	-387.19
30	30	10	49.33	-365.72	-387.36
30	40	10	49.24	-365.86	-387.37
30	50	10	49.24	-365.88	-387.37
40	10	10	46.52	-375.41	-375.41
40	20	10	51.12	-362.06	-380.38
40	30	10	50.51	-361.23	-380.38
40	40	10	50.45	-361.35	-380.35
40	50	10	50.45	-361.36	-380.35
50	10	10	47.85	-370.81	-370.81
50	20	10	52.87	-358.09	-374.76
50	30	10	52.14	-357.66	-374.62
50	40	10	52.11	-357.77	-374.64
50	50	10	52.12	-357.78	-374.63

Table 2: Parameters for case studies and the corresponding results for Winkler model

Input Data			*Results (Winkler Model)*		
N_{60}	*L* (m)	*B* (m)	Subgrade Reaction (kN/m^2)	M_{xx} (kN.m/m)	M_{yy} (kN.m/m)
10	10	10	61.64	-343.25	-343.25
10	20	10	60.68	-341.44	-343.45
10	30	10	60.70	-341.43	-343.17
10	40	10	60.70	-341.43	-343.17
10	50	10	60.70	-341.43	-343.17
20	10	10	76.46	-344.80	-344.80
20	20	10	75.69	-341.16	-344.63
20	30	10	75.95	-341.23	-344.63
20	40	10	75.95	-341.23	-344.64
20	50	10	75.95	-341.23	-344.64
30	10	10	88.30	-343.08	-343.08
30	20	10	88.12	-339.28	-342.90
30	30	10	88.12	-339.30	-342.90
30	40	10	88.12	-339.30	-342.90
30	50	10	88.12	-339.30	-342.90
40	10	10	98.48	-340.57	-340.57
40	20	10	98.48	-336.95	-340.38
40	30	10	98.47	-336.95	-340.38
40	40	10	98.47	-336.95	-340.38
40	50	10	98.47	-336.95	-340.38
50	10	10	107.44	-337.88	-337.88
50	20	10	107.53	-334.55	-337.69
50	30	10	107.53	-334.54	-337.69
50	40	10	107.53	-334.54	-337.69
50	50	10	107.53	-334.54	-337.69

During these case studies, variations in non-dimensional parameters of B/L and h/L have been achieved through increasing raft length, L, from 10m to 50m with an increment of 10m while both raft width, B, and raft thickness, h, have been kept constant with values of 10m and 0.5m respectively.

Non-dimensional parameters related to materials stiffness, namely $(k_sL)/E_c$ and ν_c/ν_s, have been varied through changing soil properties as a function of SPT value and

Paper ID: ART20171997 DOI: 10.21275/ART20171997

keeping concrete properties constant with compressive strength of f_c' equal to 28 MPa.

In terms of non-dimensional groups of (16) and (17), results have been reduced to those presented in Table 3 below, where the subscript "1" indicates results of finite element model with soil mass, while the subscript "2" indicates results of finite element model with Winkler foundation. The results indicate that Winkler model overestimates subgrade reactions while underestimates pertained bending moments in the foundation.

Table 3: Results for different case studies in terms of pertained non-dimensional groups

$\frac{q_1}{q_2}$	$\frac{M_{xx1}}{M_{xx2}}$	$\frac{M_{yy1}}{M_{yy2}}$	$\frac{k_s L}{E_c}$	$\frac{\nu_c}{\nu_s}$	$\frac{B}{L}$	$\frac{h}{L}$
0.774	1.162	1.162	0.010	1.138	1.000	0.050
0.789	1.183	1.193	0.020	1.138	0.500	0.025
0.798	1.127	1.196	0.030	1.138	0.333	0.017
0.804	1.127	1.196	0.040	1.138	0.250	0.013
0.802	1.128	1.196	0.050	1.138	0.200	0.010
0.603	1.126	1.126	0.020	0.916	1.000	0.050
0.645	1.105	1.150	0.040	0.916	0.500	0.025
0.644	1.091	1.151	0.060	0.916	0.333	0.017
0.638	1.091	1.151	0.080	0.916	0.250	0.013
0.638	1.091	1.151	0.101	0.916	0.200	0.010
0.520	1.110	1.110	0.030	0.772	1.000	0.050
0.565	1.082	1.129	0.060	0.772	0.500	0.025
0.560	1.078	1.130	0.090	0.772	0.333	0.017
0.559	1.078	1.130	0.121	0.772	0.250	0.013
0.559	1.078	1.130	0.151	0.772	0.200	0.010
0.472	1.102	1.102	0.040	0.670	1.000	0.050
0.519	1.075	1.118	0.080	0.670	0.500	0.025
0.513	1.072	1.118	0.121	0.670	0.333	0.017
0.512	1.072	1.117	0.161	0.670	0.250	0.013
0.512	1.072	1.117	0.201	0.670	0.200	0.010
0.445	1.097	1.097	0.050	0.595	1.000	0.050
0.492	1.070	1.110	0.101	0.595	0.500	0.025
0.485	1.069	1.109	0.151	0.595	0.333	0.017
0.485	1.069	1.109	0.201	0.595	0.250	0.013
0.485	1.069	1.109	0.251	0.595	0.200	0.010

5. Regression Analysis

To modify the results of traditional Winkler model to those determined based on finite element simulation of soil mass, linear regression model presented in (18) below is proposed for subgrade reactions:

$$\frac{q_1}{q_2}=\beta_{q0}+\beta_{q1}\left(\frac{k_s\times L}{E_c}\right)+\beta_{q2}\left(\frac{\nu_c}{\nu_s}\right)+\beta_{q3}\left(\frac{B}{L}\right)+\beta_{q4}\left(\frac{h}{L}\right) \quad (18)$$

By the definition of q_1 and q_2 as subgrade reactions determined based on simulation of soil mass and based on Winkler model respectively, (18) above can be re-written as indicated in (19) below:

$$q_1 = \mu_q q_2 \quad (19)$$

where μ_q is a modification factor that relates the subgrade reactions computed based on Winkler model to more accurate values that can be determined if soil mass is included in the finite element model. From (18) and (19), μ_q factor will be:

$$\mu_q = \beta_{q0} + \beta_{q1}\left(\frac{k_s\times L}{E_c}\right) + \beta_{q2}\left(\frac{\nu_c}{\nu_s}\right) + \beta_{q3}\left(\frac{B}{L}\right) + \beta_{q4}\left(\frac{h}{L}\right) \quad (20)$$

In the same approach, bending moments determined from two models can be related as follows:

$$\mu_{Mx} = \beta_{Mx0} + \beta_{Mx1}\left(\frac{k_s\times L}{E_c}\right) + \beta_{Mx2}\left(\frac{\nu_c}{\nu_s}\right) + \beta_{Mx3}\left(\frac{B}{L}\right) + \beta_{Mx4}\left(\frac{h}{L}\right) \quad (21)$$

$$\mu_{My} = \beta_{My0} + \beta_{My1}\left(\frac{k_s\times L}{E_c}\right) + \beta_{My2}\left(\frac{\nu_c}{\nu_s}\right) + \beta_{My3}\left(\frac{B}{L}\right) + \beta_{My4}\left(\frac{h}{L}\right) \quad (22)$$

Using the data of Table 3 above, regression coefficients, β_s, presented in Table 4 below have been determined by the method of least squares, [18]. Values of correlation coefficient, R^2, indicate that there are strong linear relations between results of the two models.

Table 4: Regression coefficients for linear models of (20), (21), and (22)

Regression coefficient	*Average Value determined by the method of least squares*	R^2
β_{q0}	0.130	0.982
β_{q1}	0.023	
β_{q2}	0.589	
β_{q3}	0.185	
β_{q4}	-4.62	
β_{Mx0}	0.929	0.892
β_{Mx1}	0.135	
β_{Mx2}	0.159	
β_{Mx3}	0.416	
β_{Mx4}	-7.149	
β_{My0}	1.052	0.972
β_{My1}	-0.078	
β_{My2}	0.134	
β_{My3}	0.138	
β_{My4}	-3.536	

6. Conclusions

In an attempt to modify traditional Winkler model to take shear forces between adjacent soil prisms into account in computing subgrade reactions and bending moments in raft foundations, two finite element soil simulations have been considered in this study. In the first model, Winkler simulation has been adopted while in the second one soil mass has been simulated with brick finite element.

Linear regression analyses indicate that results of two models are significantly correlated in such a way that results of Winkler model can be modified to predicate the more

Paper ID: ART20171997 DOI: 10.21275/ART20171997

accurate results without including soil mass in the finite element model.

Foundations considered in this study are raft foundations with regular columns layout and supported on dry cohesionless soils.

References

[1] Fryba, L., "History of Winkler Foundation," Vehicle System Dynamics: International Journal of Vehicle Mechanics and Mobility, 24:sup1, 7-12, 1995.
[2] Rao, N. S., Foundation Design Theory and Practice, John Wiley & Sons (Asia) Pte Ltd, 2011.
[3] Lambe, T. W., & Whitman, R. V., Soil Mechanics, SI Version. John Wiley & Sons Inc., 1979.
[4] Cook, R. D., Finite Element Modeling for Stress Analysis. John Wiley & Sons Inc., 1995.
[5] Bathe, K. J., Finite Element Procedures. PHI Learning Private Limited, 1996.
[6] Popov, E. P., Introduction to Mechanics of Solids. Prentice-Hall Inc., 1968.
[7] ACI 318, Building Code Requirements for Structural Concrete (ACI 318M-08) and Commentary. American Concrete Institute, 2008.
[8] Nilson, A. H., Darwin, D., & Dolan, C. W., Design of Concrete Structure, McGraw-Hill, 2010.
[9] Das, B. M., Principles of Foundation Engineering, 7th Edition. CENGAGE Learning, 2011.
[10] Peck, R. B., Hanson, W. E., & Thornburn, T. H., Foundation Engineering, Second Edition. John Wiley and Sons Inc., 1974.
[11] Bowles, J. E., Foundation Analysis and Design, 5th Edition, McGraw-Hill, 1997.
[12] Coduto, D. P., Foundation Design, Principles and Practices, 2nd Edition, Prentice Hall, 2001.
[13] Budhu, M., Foundation and Earth Retaining Structures. John Wiley & Sons Inc., 2008.
[14] Varghese, P. C., Foundation Engineering. PHI Learning Private Limited, 2005.
[15] Hetenyi, M., Beams on Elastic Foundation, Theory with Applications in the Fields of Civil and Mechanical Engineering. The University of Michigan Press, 1946.
[16] ACI336.2R., Suggested Analysis and Design Procedures for Combined Footings and Mats, ACI, 1988.
[17] Shames, I. H., Mechanics of Fluids, 4th Edition, McGraw-Hill, 2003.
[18] Kottegoda, N. T., & Rosso, R., Applied Statistics for Civil and Environmental Engineers, 2nd Edition, Blackwell Publishing, 2008.

Authors Profile

Salah R. Al-Zaidee received his B. Sc. in civil engineering with first rank from the University of Baghdad in 1998. While he received his M. Sc. and Ph. D. degrees in structural engineering from the University of Baghdad in 2001 and 2007 respectively. Since 2001, he involved in teaching, research, and practice of civil engineering in general and structural engineering in particular. Since 2000, he is a faculty member in the Civil Engineering Department/University of Baghdad.

Aqeel T. Fadhil earned his B.Sc. degree in civil engineering in 2007 from the University of Baghdad /Iraq. In late 2012, he obtained his M.Sc. degree in civil engineering from the University of Missouri-Columbia /USA. He has been working as a faculty member at the University of Baghdad since 2008.

Omar K. Al-Kubaisi received his B.Sc. in civil engineering with first rank from the University of Baghdad (Iraq) in 2009. In 2014, he received his M.Sc. with Honor degree in civil engineering from the University of Kansas (USA). Furthermore, he involved in practice of civil engineering in general and structural/geotechnical engineering in particular. Since 2011, he is a faculty member in the Civil Engineering Department/University of Baghdad.

Paper ID: ART20171997 DOI: 10.21275/ART20171997